

## Electrical and optical properties of GaN/Al<sub>2</sub>O<sub>3</sub> interfaces

D C Look<sup>1,2,8</sup>, R L Jones<sup>1</sup>, X L Sun<sup>3</sup>, L J Brillson<sup>3</sup>, J W Ager III<sup>4</sup>,  
S S Park<sup>5</sup>, J H Han<sup>5</sup>, R J Molnar<sup>6</sup> and J E Maslar<sup>7</sup>

<sup>1</sup> Air Force Research Laboratory, MLPS, Wright-Patterson AFB, OH 45433, USA

<sup>2</sup> Wright State University, Semiconductor Research Center, Dayton, OH 45435, USA

<sup>3</sup> Ohio State University, Department of Electrical Engineering, Columbus, OH 43210, USA

<sup>4</sup> Lawrence Berkeley National Laboratory, Materials Science Division, Berkeley, CA 94720, USA

<sup>5</sup> Samsung Advanced Institute of Technology, PO Box 111, Suwon 440-600, Korea

<sup>6</sup> Massachusetts Institute of Technology, Lincoln Laboratory, Lexington, MA 02420, USA

<sup>7</sup> National Institute of Standards and Technology, 100 Bureau Drive, Gaithersburg, MD 20899, USA

E-mail: david.look@wpafb.af.mil

Received 27 September 2002

Published 22 November 2002

Online at [stacks.iop.org/JPhysCM/14/13337](http://stacks.iop.org/JPhysCM/14/13337)

### Abstract

Hall-effect, photoluminescence (PL), cathodoluminescence (CL), and Raman scattering measurements have been used to characterize the Ga (top) and N (bottom) faces of free-standing GaN layers grown by hydride vapour phase epitaxy on Al<sub>2</sub>O<sub>3</sub>. The material near the bottom has higher carrier concentration, lower mobility, larger PL linewidths, brighter CL emission, and stronger Raman plasmon–phonon lines than the material near the top. All results are consistent with the diffusion of O from the Al<sub>2</sub>O<sub>3</sub> substrate, sometimes covering a distance of several tens of micrometres. The O donor is compensated by Ga vacancy acceptors, known to exist from positron annihilation experiments. However, Raman and CL profiling show that the poor interface region ends rather abruptly, giving excellent material near the top (Ga) face.

(Some figures in this article are in colour only in the electronic version)

### 1. Introduction

The growth of GaN on a lattice-mismatched substrate, such as Al<sub>2</sub>O<sub>3</sub>, leads to a highly defected interface region, which controls the subsequent growth of the crystal and hence has a significant effect on the resulting electrical and optical properties of the final layer. Thus, it is useful to thoroughly characterize the interface region (or interface layer) in as

<sup>8</sup> Author to whom any correspondence should be addressed (at Wright State University).

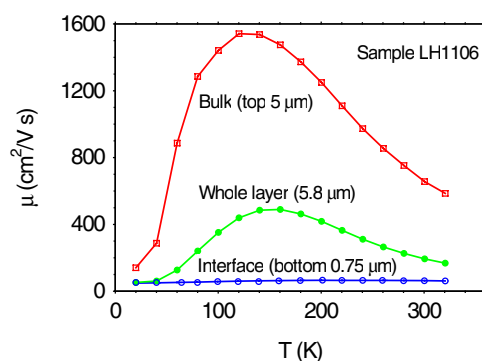


**Figure 1.** Temperature-dependent mobility of a 5.8  $\mu\text{m}$  thick HVPE layer on  $\text{Al}_2\text{O}_3$ , before and after etching off the top 5  $\mu\text{m}$ . The top curve is calculated from a two-layer model.

many ways as possible. Structural characterization is of obvious need, and indeed, techniques such as transmission electron microscopy, x-ray diffraction, and atomic force microscopy have been applied frequently and successfully. However, electrical and optical methods have seldom been employed, possibly because the interface regions are often nonconductive and nonemissive. This is especially the case for growths by molecular beam epitaxy and metal-organic vapour phase epitaxy, which typically involve a thin GaN or AlN prelayer, grown at low temperature. However, hydride vapour phase epitaxy (HVPE) of GaN on  $\text{Al}_2\text{O}_3$  usually does not employ such a prelayer, and, in fact, always results in a conductive interface layer, ranging from 0.2–50  $\mu\text{m}$  thick in samples we have investigated. This conduction can be studied with Hall-effect measurements, and analysed with degenerate electron-scattering theory [1, 2]. Also, cathodoluminescence and photoluminescence (PL) measurements show free-electron recombination as well as deep-centre recombination in interface regions [3–7], and Raman measurements detect high electron concentration and strain in interface regions [8]. Thus, electrical and optical studies can yield a rich harvest of information on GaN/ $\text{Al}_2\text{O}_3$  interfaces in HVPE material.

In past studies we have concentrated on HVPE GaN grown at Lincoln Laboratory, and have identified the dominant donors and acceptors in both the bulk and interface regions. In the present investigation, we will mainly be concerned with free-standing GaN from Samsung Corporation. It is important to note that free-standing GaN wafers may well be the future substrate of choice for a wide range of electronic and photonic GaN-based devices.

## 2. Hall-effect measurements

The conductive interface layer can profoundly influence Hall-effect data. In figure 1, we show temperature-dependent mobility for a 5.8  $\mu\text{m}$  thick HVPE/ $\text{Al}_2\text{O}_3$  GaN layer LH1106 grown at Lincoln Laboratory [9] and discussed in [10]. The middle set of data represents the as-grown layer, while the bottom set is obtained after etching off all but 0.75  $\mu\text{m}$  of the material. Clearly, the layer is not vertically homogeneous; i.e., the interface region is highly conductive, with a mobility of  $50 \text{ cm}^2 \text{ V}^{-1} \text{ s}^{-1}$ , and a carrier concentration (averaged over 0.75  $\mu\text{m}$ ) of  $1 \times 10^{19} \text{ cm}^{-3}$ . If we assume a simple two-layer model, then we can show that the top 5  $\mu\text{m}$ , the ‘bulk’ region, has the characteristics of excellent material, as shown in the upper data set. Is it reasonable to break the total layer into an interface region, of thickness  $< 1 \mu\text{m}$ , and a bulk region, the rest of the layer? For this sample and others grown in the same reactor, the answer

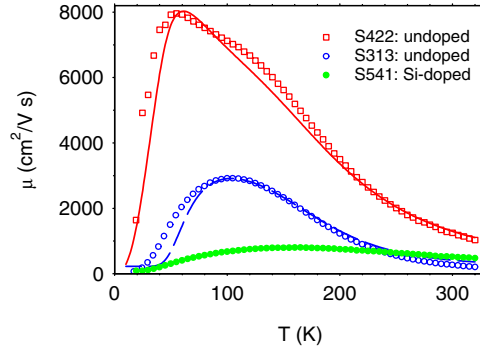


**Figure 2.** Temperature-dependent mobility for doped and undoped free-standing GaN layers. The solid curve is a fit to the data for sample S422, while the dashed curve is a fit to the S313 data assuming that S313 is identical to S422 except for the addition of a thin, degenerate layer with sheet concentration of  $5.1 \times 10^{15} \text{ cm}^{-2}$  and constant mobility of  $225 \text{ cm}^2 \text{ V}^{-1} \text{ s}^{-1}$ .

is yes, as we have shown earlier [1]. In fact, the carrier concentration  $n$ , the dislocation density  $N_{dis}$ , the Ga vacancy concentration, and the O concentration, all fall by more than two orders of magnitude within a few  $1000 \text{ \AA}$  from the interface [2]. However, an interface region this thin is not found in all HVPE growth. In a study of material from six different laboratories, we found that all HVPE layers, without exception, have a highly conductive interface layer, but that the thickness of this layer can range from  $0.2$  to  $50 \text{ }\mu\text{m}$ . In terms of interface sheet carrier concentration, the values range from  $1 \times 10^{14}$  to  $5 \times 10^{16} \text{ cm}^{-2}$ . To understand why this interface layer can have such an important effect on measured electrical properties, note that a  $10 \text{ }\mu\text{m}$  active layer with  $n = 1 \times 10^{17} \text{ cm}^{-3}$  has a sheet carrier concentration of only  $1 \times 10^{14} \text{ cm}^{-2}$ , and a typical 2DEG layer in an AlGaIn/GaN field-effect transistor structure, only about  $1 \times 10^{13} \text{ cm}^{-2}$ .

In this paper, we will be mainly concerned with free-standing GaN wafers produced by Samsung Corporation [11]. Other companies are also producing free-standing GaN wafers, because they have potential as substrates for GaN-based electronic and photonic devices. The Samsung production process involves several steps:

- (1) growth of a thick ( $\sim 500 \text{ }\mu\text{m}$ ) HVPE layer on a two-inch Al<sub>2</sub>O<sub>3</sub> wafer;
- (2) separation of the GaN layer from the Al<sub>2</sub>O<sub>3</sub>; and
- (3) flattening of the bowed GaN wafer by grinding and/or etching both the top and bottom surfaces.

For characterization purposes,  $1 \text{ cm} \times 1 \text{ cm}$  pieces are cut from the two-inch wafers. Three examples of free-standing  $1 \text{ cm} \times 1 \text{ cm}$  samples, S422, S313, and S541, are clearly delineated by their respective Hall-effect properties, as shown in figures 2 and 3. S422 is an undoped layer that demonstrates the excellent quality available from the HVPE process; this layer has a  $300 \text{ K}$  mobility  $\mu_{300}$  of  $1250 \text{ cm}^2 \text{ V}^{-1} \text{ s}^{-1}$ , a peak mobility  $\mu_{peak}$  of  $7960 \text{ cm}^2 \text{ V}^{-1} \text{ s}^{-1}$ , and fitted donor ( $N_D$ ) and acceptor ( $N_A$ ) concentrations of  $1.3 \times 10^{16}$  and  $2.5 \times 10^{15} \text{ cm}^{-3}$ , respectively. S541 is doped with Si, and has  $\mu_{300} = 520 \text{ cm}^2 \text{ V}^{-1} \text{ s}^{-1}$ ,  $\mu_{peak} = 800 \text{ cm}^2 \text{ V}^{-1} \text{ s}^{-1}$ ,  $N_D = 8.4 \times 10^{17} \text{ cm}^{-3}$ , and  $N_A = 1.4 \times 10^{17} \text{ cm}^{-3}$ , reasonable values for a doped sample. As expected,  $\mu(\text{S541}) < \mu(\text{S422})$  at every temperature. But, in contrast, note the anomalous nature of S313, which has  $\mu_{300} = 270 \text{ cm}^2 \text{ V}^{-1} \text{ s}^{-1}$  and  $\mu_{peak} = 2920 \text{ cm}^2 \text{ V}^{-1} \text{ s}^{-1}$ , giving  $\mu_{300}(\text{S313}) < \mu_{300}(\text{S541})$ , but  $\mu_{peak}(\text{S313}) > \mu_{peak}(\text{S541})$ . This strange behaviour can only be explained by the existence of a highly conductive layer in S313, evidently not all etched

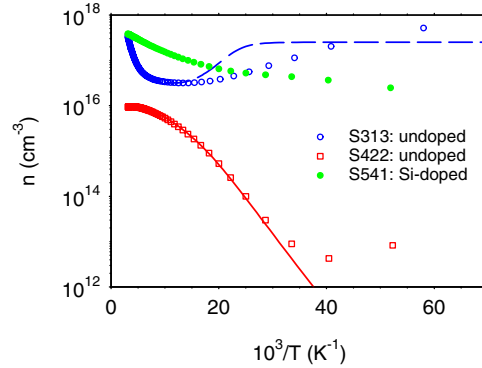


**Figure 3.** Temperature-dependent electron concentrations for doped and undoped free-standing GaN layers. The solid curve is a fit to the data for sample S422, while the dashed curve is a fit to the S313 data assuming that S313 is identical to S422 except for the addition of a thin, degenerate layer with sheet concentration of  $5.1 \times 10^{15} \text{ cm}^{-2}$  and constant mobility of  $225 \text{ cm}^2 \text{ V}^{-1} \text{ s}^{-1}$ .

off during the flattening process. In fact, if we take the fitted S422 data, shown as solid curves in figures 2 and 3, and then just use a simple two-layer model to artificially add another layer, with sheet concentration  $5.1 \times 10^{15} \text{ cm}^{-2}$  and mobility  $225 \text{ cm}^2 \text{ V}^{-1} \text{ s}^{-1}$ , we get the dashed curves in figures 2 and 3, which turn out to give a good fit to S313, for  $T > 80 \text{ K}$ . The fit below  $80 \text{ K}$  is not as good, probably because the actual interface layer in S313 is not truly degenerate (temperature independent), as it was for LH1106, discussed above. However, the overall quality of the fit clearly shows that S313 has a good bulk region, comparable to that of S422, and a poor interface region.

The preceding comparison of S313 and S541 shows that the  $300 \text{ K}$  values of  $n$  and  $\mu$  are not always good indicators of sample quality. For example, even though  $n_{300}$  is about the same for S313 and S541, the *bulk* region of S313 contains much better material than that of S541. Are there any easy ways to identify the existence of a conductive interface layer, such as that found in S313? In figure 3, note the steep slope of the  $\log(n)$  versus  $1/T$  curve near room temperature. That is, for a *uniformly* conductive layer, controlled by a shallow donor, the slope should *never* be larger than about  $30 \text{ meV}$ , and if  $n > 10^{17} \text{ cm}^{-3}$ , not larger than about  $20 \text{ meV}$ . Thus, S422 and S541 are ‘normal’, homogeneous undoped and doped layers, respectively, while S313 has anomalous characteristics because of its interface layer. The optical properties are also anomalous, as shown below.

### 3. Photoluminescence

Samples such as S313 display  $4.2 \text{ K}$  PL spectra of the type shown in figures 4 and 5. Excitation was provided by a  $45 \text{ mW}$  HeCd laser, and resolution was at least a factor of 20 better than the width of the narrowest line in a particular spectrum. The strongest PL lines arise from the collapse of donor-bound excitons ( $\text{D}^0\text{Xs}$ ), and these spectra are shown in figure 4. For the N face, the side originally closest to the  $\text{Al}_2\text{O}_3$  substrate, the  $\text{D}^0\text{X}$  line is quite broad, as would be expected from highly conductive material. On the other hand, the Ga-face  $\text{D}^0\text{X}$  spectrum has an intense sharp line at  $3.472 \text{ eV}$ , probably due to  $\text{O}_\text{N}$ , and a weaker line at  $3.473 \text{ eV}$ , perhaps related to  $\text{Si}_\text{Ga}$ . Such a large difference in Ga-face and N-face  $\text{D}^0\text{X}$  linewidths is not seen for sample S422 (not shown), because in that sample, most of the interface layer has been removed. For the deep-centre spectral lines of S313 (figure 5), the linewidths are similar, but there are differences

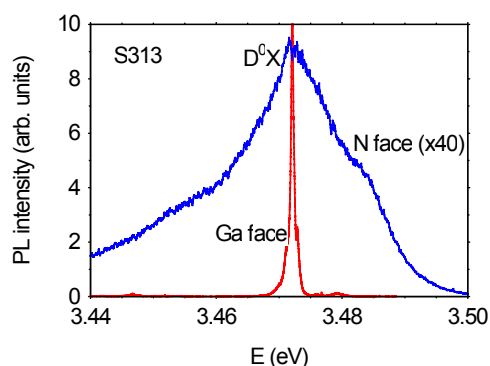


**Figure 4.** Donor-bound-exciton ( $D^0X$ ) PL spectra (4.2 K) of the Ga and N faces of S313, a sample with a degenerate interface layer (N face).

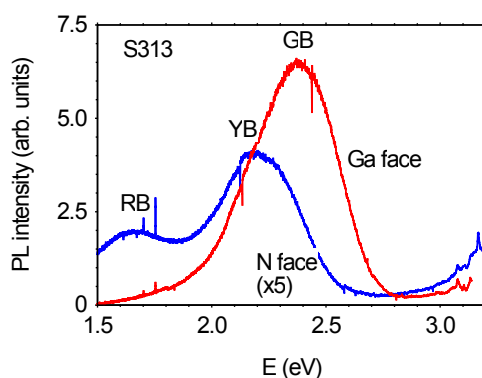


**Figure 5.** Deep-centre PL spectra (4.2 K) of the Ga and N faces of S313, a sample with a degenerate interface layer (N face). Shown are the GB (green band), YB (yellow band), and RB (red band).

in the energies [6, 7]. As stated earlier, the N face should have higher concentrations of O and  $V_{Ga}$ , because O diffuses from the Al<sub>2</sub>O<sub>3</sub>, and  $V_{Ga}$  acceptors are probably formed in response to the O donors (self-compensation). Since the yellow band (YB) is thought to involve  $V_{Ga}$  centres, it is, at first glance, not surprising that this band is more dominant in the N-face spectrum. However, the other deep centres may also involve  $V_{Ga}$ . Indeed, considering the growth temperatures, the  $V_{Ga}$  defects are most probably not isolated, but rather complexed with donors, such as  $O_N$ . The differences between the YB and green band (GB) may then be the number of O atoms complexed with a given  $V_{Ga}$ , and if so, our data would suggest that the YB should have a higher O complexity. That is, the GB might involve  $V_{Ga}-O_N$ , and the YB,  $V_{Ga}-(O_N)_2$ . The red band, then, might be associated with  $V_{Ga}-(O_N)_3$  centres. All of these  $V_{Ga}-(O_N)_n$  ( $n = 1-3$ ) centres should be stable in n-type material, according to theory [12]; however, their existence has not been proven, and thus the present model should be viewed as pure speculation.

#### 4. Cathodoluminescence imaging

Cathodoluminescence (CL) is a powerful method of obtaining emission spectra because of the large density of electron-hole pairs produced by an electron beam [4, 5]. One advantage of this high density is that good emission intensities can often be obtained even at room

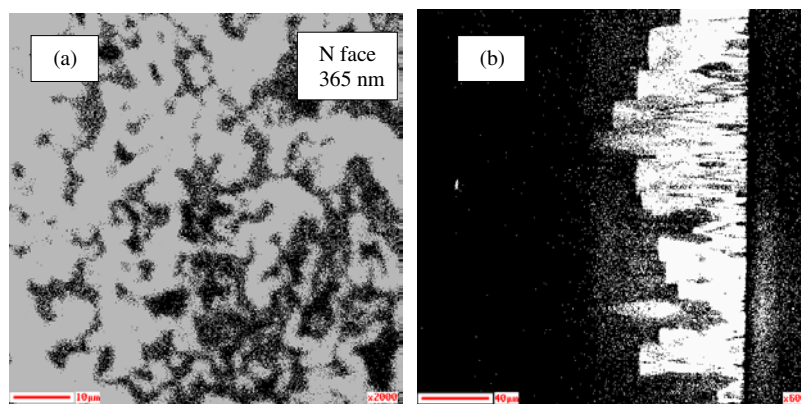


**Figure 6.** Room-temperature, 365 nm CL images of S389. (a) N face, plan view; (b) cross-sectional view, with the N face on the right. The Ga-face plan view (not shown) is relatively featureless.

temperature. Also, when combined with scanning electron microscope optics, detailed images can be obtained. In figure 6 is displayed a room-temperature, cross-sectional CL image of S389, a sample which is similar to S313. Note the bright columnar features emanating a few tens of micrometres from the N face. In GaN, such bright CL regions are usually associated with highly conductive material, most probably due to O donors diffusing from the  $\text{Al}_2\text{O}_3$  substrate. Indeed, it is this high-concentration, low-mobility interface region that leads to the anomalous Hall-effect results for LH1106 (figure 1) and S313 (figures 2 and 3). However, it should be emphasized that the material above the interface region of each of these samples, all the way up to the Ga face, is excellent, as typified by the sharp PL lines on the Ga face (figure 4), and the high ‘bulk’ mobility as shown by the two-layer Hall fits (figures 1 and 2).

## 5. Raman spectroscopy

The prominent Raman features in high-quality, low-conductivity GaN, for the case of parallel polarizations of the incident and scattered radiations, are the  $E_2$  and  $A_1(\text{LO})$  lines. However, for highly conductive samples (say,  $n \geq \text{mid-}10^{17} \text{ cm}^{-3}$ ), the  $A_1(\text{LO})$  and plasmon modes interact and form new modes, designated  $L_+$  and  $L_-$ . The intensity of the LO mode is dependent upon  $n$  [8], and various formulae have been developed to quantify this relationship. In figure 7, we have plotted the intensity ratio  $A_1(\text{LO})/E_2$  as a function of the focus position of a 488 nm laser beam, having about  $1 \mu\text{m}$  lateral resolution. For this experiment, a depth resolution of about  $25 \mu\text{m}$  is estimated. Clearly the  $A_1(\text{LO})/E_2$  ratio decreases in the region close to the interface, a phenomenon caused by the higher carrier concentration in this region. Note that the length scale associated with the increase in  $n$  is several tens of micrometres, consistent with that of the cross-sectional CL image, shown in figure 6(b). Plan-view Raman images (not shown) are also consistent with plan-view CL images of the Ga and N faces, such as the CL image shown in figure 6(a).

## 6. Discussion

The data presented above show that HVPE GaN/ $\text{Al}_2\text{O}_3$  interface regions can range from  $<1 \mu\text{m}$  thickness (figure 1) to  $>10 \mu\text{m}$  (figures 6(b) and 7). However, in each case, the material near the top (Ga face) is of high quality. Earlier [2] we had pointed out the strong spatial

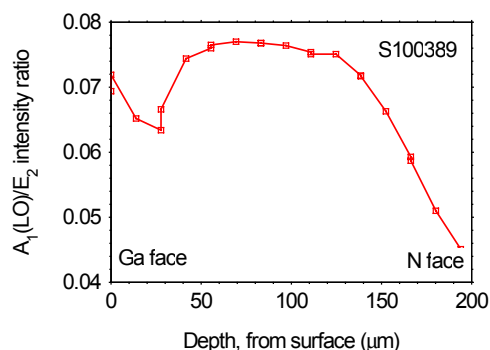


**Figure 7.** The ratio of the intensities of the A<sub>1</sub>(LO) (or L<sub>+</sub>) and E<sub>2</sub> Raman modes for sample S389. The depth resolution is about 25 μm.

correlation between the dislocation density  $N_{dis}$ , and other quantities, such as [O],  $n$ ,  $N_D$ ,  $N_A$ , and  $[V_{Ga}]$ , near the interface of samples such as LH1106 (figure 1). In the Samsung samples, the immediate interface region is not directly observed because of the flattening process. However, in cases for which a high-conductivity region still exists near the N face, such as for S313, the value of  $N_{dis}$  will also be significantly higher there. In the very best material, with  $\mu_{peak} > 8000 \text{ cm}^2 \text{ V}^{-1} \text{ s}^{-1}$ ,  $N_{dis}$  is very low,  $\leq 2 \times 10^6 \text{ cm}^{-2}$ . Thus, low values of dislocation density seem to be correlated with low donor and acceptor concentrations, and vice versa. Such a phenomenon is certainly not new, and in past literature has even fostered terms such as ‘pipe diffusion’ and ‘Cottrell atmosphere’. But the data given here show that these concepts also apply to GaN grown on Al<sub>2</sub>O<sub>3</sub>.

The reasons for the correlation between dislocations and impurity/defect diffusion are not fully known, although one commonly invoked mechanism is diffusion enhancement in the dislocation strain field [12]. However, it is also important to consider the formation energies of the various point defects and impurities. That is, in the presence of donors, the formation of native acceptors is more probable, especially in wide-gap materials [13]. We also know that the threading dislocations in strongly n-type GaN are negatively charged, and that  $V_{Ga}$  concentrations are high in the regions of high  $N_{dis}$  [2]. In fact, a dislocation can act as a giant acceptor by forming  $V_{Ga}$  centres along its core [12, 14]. Thus, the diffusion of O donors will possibly promote dislocations with  $V_{Ga}$  cores, or vice versa. Or, the dislocations may have full cores [15], but negatively charged Cottrell atmospheres [12]. Clearly, the system must be viewed in its entirety, with available defects and impurities as well as their potential charge states taken into account. As discussed above, optical and electrical characterizations have already been used, along with structural characterization, to help sort out the issues. However, more progress will be possible if ‘fingerprints’ can be established for some of the defects and impurities involved. For example, we still do not know the microscopic identifications of the blue, green, yellow, and red luminescence bands, mentioned earlier. Theory has been, and will continue to be, very important in identifying the various species, because theoretical and experimental energies and concentrations must be consistent. In the end, a full understanding of the GaN/Al<sub>2</sub>O<sub>3</sub> interface will probably suggest modifications of the growth processes leading to improved material.

### Acknowledgments

We wish to thank T A Cooper for the electrical measurements and W Rice for the PL measurements. DCL was supported under United States Air Force Contract F33615-00-C-



5402 and AFOSR Grant F49620-00-1-0347. LJB and XLS were supported under ONR Grant N00014-00-1-0042. The work at LBNL was supported by the Directorate, Office of Science, Office of Basic Energy Sciences, Division of Materials Sciences and Engineering, of the US Department of Energy under Contract No DE-AC03-76SF00098. The Lincoln Laboratory portion of this work was sponsored by the ONR under Air Force contract No F19628-00-C-0002. Opinions, interpretations, conclusions, and recommendations are those of the authors and not necessarily endorsed by the United States Air Force.

## References

- [1] Look D C and Molnar R J 1997 *Appl. Phys. Lett.* **70** 3377
- [2] Look D C, Stutz C E, Molnar R J, Saarinen K and Liliental-Weber Z 2001 *Solid State Commun.* **117** 571
- [3] Arnaudov B, Paskova T, Goldys E M, Yakimova R, Evtimova S, Ivanov I G, Henry A and Monemar B 1999 *J. Appl. Phys.* **85** 7888
- [4] Paskova T, Goldys E M, Yakimova R, Svedberg E B, Henry A and Monemar B 2000 *J. Cryst. Growth* **208** 18
- [5] Sun X L, Goss S H, Brillson L J, Look D C and Molnar R J 2001 *Phys. Status Solidi b* **228** 441  
Goss S H, Sun X L, Young A P, Brillson L J, Look D C and Molnar R J 2001 *Appl. Phys. Lett.* **78** 3630
- [6] Freitas J A Jr, Braga G C B, Moore W J, Tischler J G, Culbertson J C, Fatemi M, Park S S, Lee S K and Park Y 2001 *J. Cryst. Growth* **231** 322
- [7] Reshchikov M A, Morkoç H, Park S S and Lee K Y 2001 *Appl. Phys. Lett.* **78** 3041
- [8] Matthews M J, Hsu J W P, Gu S and Keuch T F 2001 *Appl. Phys. Lett.* **79** 3086
- [9] Molnar R J, Maki P, Aggarwal R, Liau Z L, Brown E R, Melngailis I, Götz W, Romano L T and Johnson N M 1996 *Mater. Res. Soc. Symp. Proc.* **423** 221
- [10] Look D C, Hoelscher J E, Brown J L and Via G D 2001 *MRS Internet J. Nitride Semicond. Res.* **6** 10
- [11] Oh E, Lee S K, Park S S, Lee K Y, Song I J and Han J Y 2001 *Appl. Phys. Lett.* **78** 273
- [12] Elsner J, Blumenau A Th, Frauenheim T, Jones R and Heggie M I 2000 *Mater. Res. Soc. Symp. Proc.* **595** W9.3.1
- [13] Neugebauer J and Van de Walle C G 1994 *Phys. Rev. B* **50** 8067
- [14] Wright A F and Grossner U 1998 *Appl. Phys. Lett.* **73** 2751
- [15] Xin Y, James E M, Arslan I, Sivananthan S, Browning N D, Pennycook S J, Omnès F, Beaumont B, Faurie J-P and Gibart P 2000 *Appl. Phys. Lett.* **76** 466